The Behavior of Steel Perimeter Columns in a High-Rise Building under Fire

MARIA M. GARLOCK and SPENCER E. QUIEL

Steel construction practice circa 1970 required a larger fire-resistance rating for members supporting more than one floor, as is the case with most columns, than for members that support only one floor, as is the case with most beams (BOCA, 1969). One basis for requiring a larger fire rating for columns is that the failure of one column can result in the collapse of multiple levels of a structure (a disproportionate collapse), whereas failure of a beam may cause a localized partial collapse. In the plane perpendicular to the exterior wall, a perimeter column is typically laterally braced by one beam. The fire-induced structural response of this beam that frames into the perimeter column directly affects the perimeter column behavior and the structural integrity of the frame as a whole. Recent codes (ICC, 2000) appropriately require equal fire protection requirements for these beams to the columns. This research evaluates the interaction between the perimeter column and the beam that frames into it through a study of a steel high-rise building subjected to a large fire. A two-dimensional model of eleven upper level floors of a steel-framed high-rise building subjected to fire is analyzed. The computational model considers the transient action of the fire (it considers that some floors are cooling down while others are heating up).

The Meridian Bank Building in Philadelphia, PA, otherwise known as the One Meridian Plaza (1MP), is the prototype building used in this study. On February 23, 1991, at approximately 8:00 p.m., a fire started on the 22nd floor of 1MP. Firefighting activities were hampered by a loss of electrical and emergency power, inadequate water pressure, and other issues (Klem, 1991; FEMA, 1991). Consequently, the fire spread to the 30th floor where it was stopped by the automatic sprinkler system, which was not yet installed in the other fire-burning floors. The fire burned for more than 18 hours and completely burned out eight floors near the top of this 38-floor structure (Klem, 1991). No structural collapse ensued and the building was dismantled in 1999. This research is not a study of the 1MP fire event per se, but rather it uses this structure and fire as a prototype for the study.

1MP was rectangular in plan and approximately 74 meters by 28 meters (243 ft by 92 ft) as shown in Figure 1. The building construction was structural steel with a slab over a metal deck. The construction required 2-hour fire rated beams and 3-hour fire rated columns, specified by the Philadelphia Department of Licenses and Inspections as equivalent to BOCA Type 1B construction (FEMA, 1991). All structural steel beams and metal decks were protected with spray-on fire resistive material (SFRM). The columns were protected with the same SFRM as well as gypsum plaster boards. The structural system consisted of several moment-resisting frames (MRFs) running in the north-south and east-west directions on every column line as shown in the floor plan in Figure 1. Enclosed private offices were typically located along the building perimeter except along the south wall where the core was located. Most of the other space was open.

An analysis of the effects of the fire on the 1MP structure was previously performed by Dexter and Lu (2001). Their study assessed the structural integrity of the steel moment frame as it existed after the fire and did not consider a thermal analysis. In contrast, our study evaluates the performance of the structure during its exposure to the 1991 fire. Two-dimensional analyses of high-rise steel buildings under fire have been recently performed by Usmani, Chung, and Torero (2003), and researchers at the National Institute of Standards and Technology (NIST, 2004) as applied to several stories of the World Trade Center (WTC). The objective of these studies was to develop a better understanding of the mechanical response of the WTC frame and possible collapse mechanisms. These studies demonstrated the usefulness of two-dimensional frames to illustrate the structural interaction of perimeter columns with a heated floor system. However, the WTC structural system is unique because of its lightweight steel-trussed floor system and perimeter column

Maria M. Garlock is assistant professor, Princeton University, department of civil and environmental engineering, Princeton, NJ.

Spencer E. Quiel is graduate student, Princeton University, department of civil and environmental engineering, Princeton, NJ.

tube construction; the results therefore have limited applications to structures of more common steel construction such as MRFs with wide-flange beams. The prototype selected for our study represents a fairly common structural system for a high-rise steel building constructed around the same time as the WTC. The conclusions are therefore relevant to many steel high-rise structures.

DEFINING THE FIRE

The fire model used in the analyses is intended to represent a reasonable approximation and simplification of the 1MP fire event. Based on observations, the 1MP fire engulfed nearly the entire floor area of floors 22 through 29; that is, it was not contained in an office space/compartment. Therefore, widely used fire time-temperature numerical models cannot be solely used to represent this fire since the scale of the 1MP fire falls well outside the scale and limitations of these models. Accordingly, the fire model used in these analyses is based on a compartment fire model as well as data from large compartment fire tests and observations during the actual fire. The fire model for each of the individual floors was developed as a three phase curve: (1) a fire growth phase with a quick rise in temperature; (2) a constant temperature phase when the fire is assumed to remain at its maximum intensity as it continues to consume fuel; and (3) a decay phase in which the fire temperatures cool as the fuel becomes exhausted.

Eurocode compartment fire models (EC1, 1994), modified by Buchanan (2002), were used to approximate the maximum temperature, T_{max}, reached on the floors and the initial rate of temperature rise. These models produce a time-temperature relationship that defines a ventilation controlled fire based on the compartment size, fuel load, ventilation openings, and compartment lining materials. For the purposes of determining T_{max}, a compartment size equal to the tributary area of the 2-D frame section considered for this study was selected. In a typical office space, the materials on the walls, floors, and ceiling would be a combination of gypsum plaster and concrete. Two Eurocode estimations for T_{max} were made based on a single insulation material input: one for gypsum plaster lining and another for concrete lining. The average of these two estimations leads to the selection of T_{max} equal to 1000 °C (1,832 °F). This temperature is consistent with the estimated maximum temperature reached in the WTC towers according to a study by researchers at NIST (McGrattan, Bouldin, and Forney, 2005), whose studies were based upon experimental compartment fires and computational fluid dynamics models.

The heating rate of the fire on each floor was based on the Eurocode (EC1, 1994) with modifications recommended by Buchanan (2002) in which case the compartment temperature reaches 725 °C (1,337 °F) in 4 minutes and T_{max} in 20 minutes. The decay rate of the fire was based on observed rates in large compartment fires. Kirby, Wainman, Tomlinson, Kay, and Peacock (1999) tested large-scale compartment fires in a 23-meter-long by 6-meter-wide by 3-meter-high (75.5 ft by 19.7 ft by 9.8 ft) space where decay rates of roughly 7 °C (44.6 °F) per minute were observed (less than that predicted by the Eurocode equations). Further experimental data (Kawagoe, 1958) showed that the decay rate of a fire with a fully developed period of more than one hour is approximately 7 °C (44.6 °F) per minute as well. In our study, we assumed a slower decay rate than those observed in the experiments referenced above since this fire was of a greater duration. A decay rate of 5 °C (41 °F) per minute was therefore selected, which results in a time-history of the fire that is consistent with the observations during the actual 1MP fire as described below.

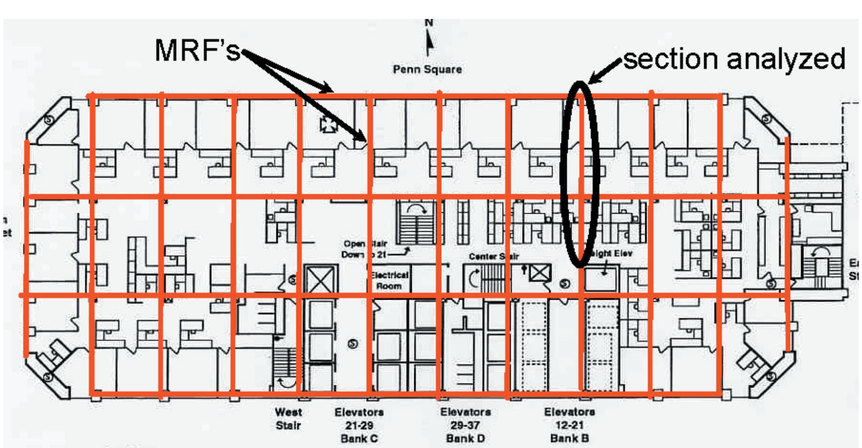

Fig. 1. Floor plan of One Meridian Plaza (FEMA, 1991).

Figure 2 shows the time-history of the floor fires used in the analyses, which starts on Floor 22 and progresses to the next floor every 1.75 hours. Each floor is subjected to the model fire described previously. The time history of the fire is consistent with eyewitness observations during the 1MP fire. For example, Dexter and Lu (2001) indicate that the fire was burning in as many as three floors at one time. Also, Klem (1991) indicates that about 5.5 hours after ignition, the fire had spread from Floor 22 through Floors 23 and 24 and was beginning to threaten Floor 25. Klem (1991) also indicates that 18.5 hours after the fire began sprinklers were activated on Floor 30, which finally halted the vertical progression of the fire.

COMPUTATIONAL MODEL

Figure 1 shows a plan view of the location of the moment frame, oriented in the N-S direction, which was selected for our study. Figure 3 shows an elevation of the symmetrically modeled prototype MRF used for two-dimensional analyses. The model includes the portion of the 1MP building affected by the fire: the twenty-first floor up to the thirty-third floor. Dimensions, member sizes, and fire protection material details of the frame were obtained from the original design drawings. Only one full bay (drawn in dark lines) is subject to fire loads. The one-half bay (drawn in light lines) is used to model rotational rigidity at the beam-column connection at the interior column. The plan view in the lower right-hand corner of Figure 3 (Section a-a) indicates that the columns bend about the strong axis in the plane of the model. The base of the modeled sub-structure is fixed against rotation and translations. Because this boundary is sufficiently far away from the fire affected zone, these restraints do not have a significant influence on the results. At the MRF centerline, the beams are fixed against rotation and lateral translation, modeling a plane of symmetry in the structure. The vertical translation of these nodes is slaved to the vertical translation

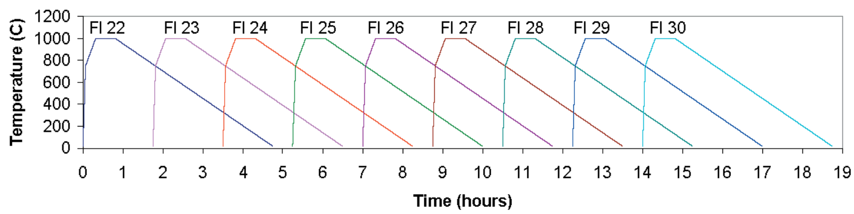

Fig. 2. Time-history of fire progression assumed in analysis.

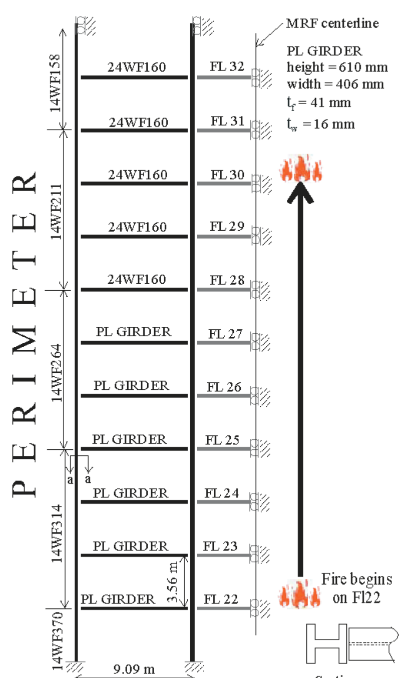

Fig. 3. Elevation of the 2-D computational model.

Table 1: Specifications for the fire protection material in 1MP.			
Temperature (°C)	Thermal Conductivity (W/mK)	Specific Heat (J/kgK)	Density (kg/m^3)
20	0.059	862	240
204	0.076	1008	240
399	0.120	1272	240
1093	0.290	1464	240

of the respective node on the interior column in order to reflect the fact that vertical elongation of the structure supporting these nodes should be similar to the thermal elongation of the interior columns. The top of both the perimeter and interior column are modeled as restrained against rotation and horizontal translation, but are free to translate vertically. The beams are connected to the column with master-slave relationships that model the column depth and clear span of the beams (the translation and rotation of the beam node is constrained to that of the column node, which has a horizontal offset from the beam node equal to one-half the column depth). While this constraint does not capture the vertical displacement that develops in the beam node due to column rotation, analyses show that this displacement would be less than 5 mm (0.2 in.) due to the small column node rotation and column depth. In addition, a separate analysis shows that if a rigid cold element were placed between the column node and beam node to act as a rigid link (instead of constraining these nodes), no visible difference in the results are seen.

The computer program SAFIR (Franssen, 2005) was employed to perform uncoupled thermal and structural analyses. In the thermal analyses, the cross section of each member is discretized into several elements (fibers), and a user-defined fire (equal to that shown in Figure 2) is imposed on the appropriate boundaries. The output is a time-temperature history at every fiber of the member cross-section. The structural analysis reads the temperature of each fiber and translates this information into mechanical response. SAFIR 2004 offers the capability of a dynamic analysis using a modified version of the Newmark-beta method, which allows the program to continue its solution beyond the point at which material or geometric instabilities may emerge (Franssen and Gens, 2004). Since the governing equation includes the mass of the structure, the solution can withstand local instabilities and large deflections.

A thermal and structural study was performed to determine the necessary level of element discretization in the beam and column cross-section. As a result, the beam flanges and web were modeled with one fiber through the *thickness*, whereas the column flanges and web were modeled with two. Several fibers were used to represent the *width* or *height* of the flanges and web. The beam and column sections contained a total of 62 fibers and 124 fibers, respectively. The structural analysis used beam elements to model the beams and columns of the frame. Ten elements represented each column story, and twenty elements represented each beam in one bay. Point loads were applied at the top of each column to represent the load applied by the floors and columns in the floors above. The load on the perimeter column was half that of the interior column since it carried half the tributary floor area.

Our analyses are intended to represent a best estimate of the *behavior* of a high-rise structure under fire loads; it is not intended for design. For this reason, the gravity loads imposed on the frame represented the full dead load (DL) and 25% of the design live loads (LL) on 1MP, which are best estimate approximations of actual loads in an office building during a fire event. This load combination is consistent with the World Trade Center study where "25% of design live load was selected as a reasonable approximation of the load that likely existed at the time of the collapse" (Zarghamee, Bolourchi, Eggers, Erbay, Kan, Kitane, Liepins, Mudlock, Naguib, Ojdrovic, Sarawit, Barrett, Gross, and McAllister, 2005). This live load percentage is also consistent with a survey of existing live loads in office buildings (Culver, 1976). The same analyses that will be discussed in this paper were repeated with a load combination of $DL + 0.50LL$ to evaluate the effects of increased live loads on the results. Both load combinations produced essentially the same results; the only major difference is that the time to failure was decreased two to three minutes in the analyses with 50% live load. It is noted that if a structure were to be designed for fire, Appendix 4 in the AISC *Specification for Structural Steel Buildings* (AISC, 2005) provides the following load combination,

$$[0.9 \text{ or } 1.2]DL + T + 0.5LL + 0.2S$$

where T and S represent the fire load and snow load, respectively. In addition, the commentary for extraordinary events in *Minimum Design Loads for Buildings and Other Structures* (ASCE, 2005) provides a similar load combination.

Each layer of fire protection material was modeled with three layers of fibers through its thickness, representing a total thickness of 39 mm (1.5 in.) for the SFRM and 19 mm (0.75 in.) for the gypsum plaster. The thermal analysis used two-dimensional solid elements. The thermal conductivity and specific heat of the steel as well as the SFRM were modeled as temperature-dependent. The material properties of steel varied according to the Eurocode (EC3, 2001). Table 1 shows the SFRM properties as a function of temperature. The plaster boards were modeled as having constant thermal conductivity (0.2 W/m-K or 0.12 Btu/h-ft-ºR), specific heat (1700 J/kg-K or 0.41 Btu/lbm-ºR), and density (800 kg/m^3 or 50 lbm/ft^3).

If the fire was on floor "x", the user-defined fire was applied to three sides of the beam on floor "x + 1", the underside of the slab on floor "x + 1", and the top of the slab on floor "x". Where the slab was not explicitly modeled, the steel beam did not have fire applied to the flange top surface, which was considered as an adiabatic surface. The perimeter columns did not have fire applied to their exterior face and the interior column had fire applied on all sides. While Figure 2 indicates that the fire in the structure lasted about 18.5 hours, the analysis continued for several hours after the fire, with the gas at ambient temperature to permit adequate time for cooling of the sections.

SAFIR uses material strength and stiffness properties at high temperatures that are based on Eurocode specifications (EC3, 2001). For example, the yield stress is multiplied by $k_{y,\theta}$, a yield stress reduction factor that becomes less than 1.0 when temperatures exceed 400 °C (752 ºF). Similarly, the Eurocode provides a reduction factor for the modulus of elasticity, $k_{E,\theta}$, which becomes less than 1.0 when temperatures exceed 100 °C (212 ºF). The stress-strain relationship, which is elastic perfectly plastic at room temperature, is transformed into a nonlinear relationship at elevated temperatures (the proportional limit stress no longer equals the yield stress). This nonlinearity begins when temperatures exceed 100 °C (212 ºF) as represented by $k_{p,\theta}$, which equals the proportional limit stress divided by the yield stress at ambient temperature. The plot of all three reduction factors versus steel temperature, as specified by the Eurocode, is provided in Figure 4.

The computational model has the following limitations/assumptions:

- Heat transfer is considered to be two-dimensional through the member cross-sections. Our analyses do not conduct heat along the length of a member or to an adjacent member. For example, when the fire is on Floor 23 but not yet on Floor 24, the heated column on Floor 23 does not conduct heat to the cold, adjacent column on Floor 24. The column on Floor 24 remains cold until the fire ignites on that floor. Likewise, the heated column is not cooled via conductive heat transfer to the adjacent cool members.

- All fire protection material remains intact throughout the duration of the fire.

- The structural analyses are two-dimensional. This is justified by the fact that, in the out-of-plane direction, the columns are braced at every floor by the spandrel beams. A separate study has shown that in our prototype building the perimeter column strength is not controlled by out-of-plane buckling since the column slenderness ratios, *L*/*r*, are small.

Representing the Slab

In our prototype, a 64-mm (2.5-in.) slab sits on a metal deck with 76-mm (3-in.) deep corrugations. The concrete was modeled with a compressive strength of 25 MPa (3.6 ksi) and zero strength in tension. The rebar and metal deck are neglected. Because the ribs of the slab are parallel to the beam, our model uses a 100-mm (4-in.) slab representing its average thickness. It is assumed that the effective with of the slab is 2.0 m (6.6 ft), based on ¼ of the clear span length of the beam (ACI, 2002). Figure 5 shows the finite-element cross section of the protected beam with the slab used for this analysis. The slab was discretized into seven fibers through its depth and 35 fibers along its total width (with finer discretization near the beam flange). The beam discretization described previously was also used for this analysis case.

The objective of this portion of the study was to determine the most efficient and appropriate means of representing the slab in a two-dimensional (2-D) analysis. To this end, two criteria were evaluated: (1) the *structural effect* that the slab has on the perimeter column deformation and resulting bending moments, and (2) the *thermal effect* of modeling the beam plus slab with fire applied on all sides, compared to modeling the beam (no slab) with the fire applied on three

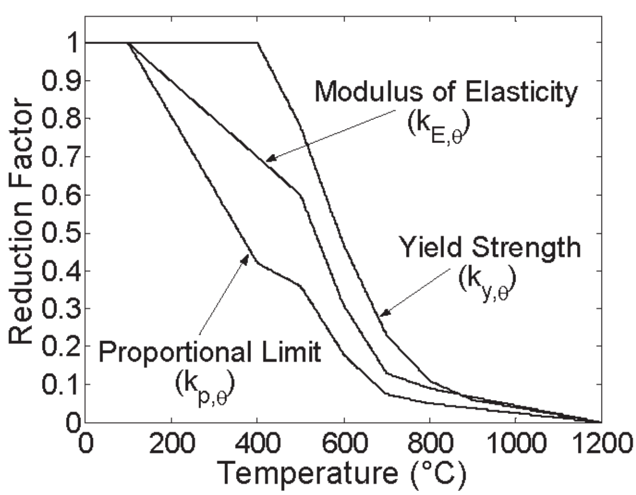

Fig. 4. Reduction factors for the material properties of structural steel (EC3, 2001).

sides (not applied to the top surface of the beam flange). In the latter case, the assumption is that the slab prevents heat transfer to the beam supporting it.

To accomplish the first objective, a beam plus slab model (named BpCp-slab) was developed as described above and subjected to a thermal analysis. This thermal analysis result was input into two different structural models: The first model used the true mechanical properties of the concrete slab (the slab is structurally *active*), and the second model used the mechanical material properties of "insulation", which has no structural capacity, for the slab (the slab is structurally *inactive*). In this manner, the thermal response of the steel beam is the same in both models yet the structural response will be different, thus permitting an evaluation of the structural effects of the slab. Figure 6 shows the evolution of the lateral deformation, Δ, of the column at its interface with Floor 23 for both structural models. The results are nearly identical as the slab produces only 3.4% of added Δ, which is due to the added thermal expansion of the concrete. Since the amount of moment developed in the column is mostly due to the column deformation, Δ, the slab's effect on the moment developed in the perimeter column is also negligible. Structurally, the slab does affect the beam vertical displacement, as the model with the slab active has smaller beam displacements than the model with the slab inactive. However, these differences in beam displacements do not affect the perimeter column behavior and overall frame stability.

To accomplish the second objective, we compared the thermal response of the beam in the BpCp-slab model versus that of a model with no slab, but the steel beam did not have fire applied to the top surface of the beam flange (named BpCp). Since the latter model did not explicitly model the slab but instead had the fire applied on three sides of the beam, the model assumes that the slab prevents heat transfer to the beam supporting it. Figure 7 compares the weighted average temperatures of these two models for the protected beam on Floor 23. The beam in model BpCp-slab reached a maximum temperature about 20 °C (68 ºF) greater than the beam in model BpCp, representing a difference of less than 6%. This temperature difference has an insignificant affect on the structural results.

These results of the slab study suggest that in a 2-D analysis of a high-rise MRF, representing the slab with finite elements has a negligible effect on the perimeter column moments and deformations. This is because the edges of the slab are not restrained in a 2-D analysis and are therefore free to expand and contract. This study also shows only a small difference in the average beam temperature between the two thermal models (the model with the beam plus slab and fire on all sides versus the model with the beam and no slab with the fire not applied to the top flange of the beam). These results indicate that in 2-D thermal and structural

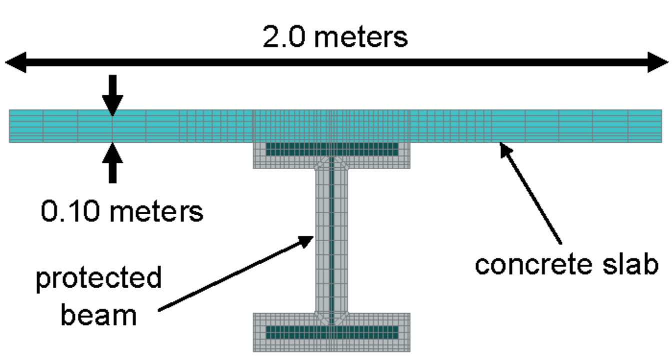

Fig. 5. Representative cross-section of a fireproofed steel floor beam with a concrete slab.

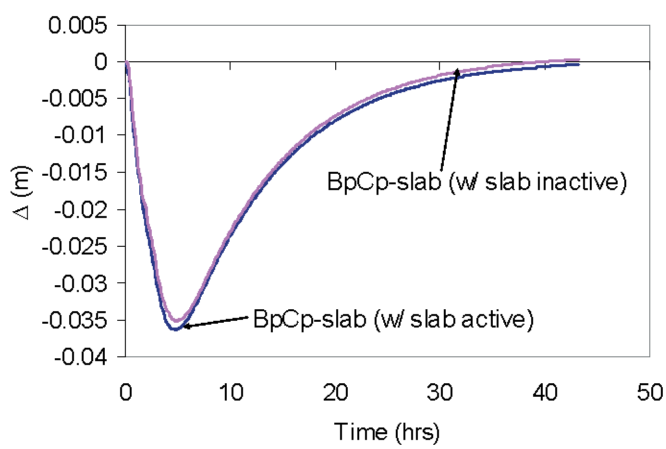

Fig. 6. Column lateral deflection, Δ, magnified 20 times, for the BpCp-slab case plotted for the active and inactive slab cases at Floor 23.

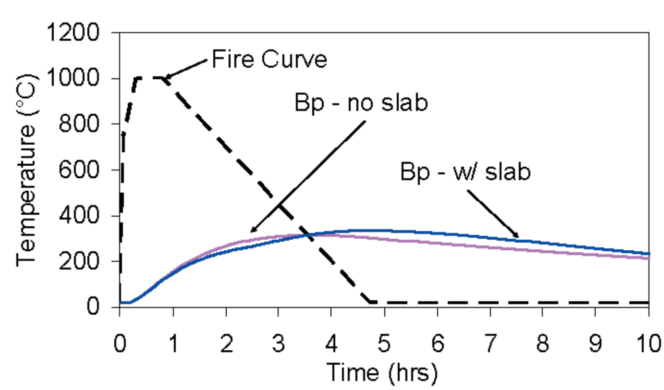

Fig. 7. Applied fire curve and weighted average Floor 23 beam temperature for the case with and without a slab included in the thermal model.

models it is reasonable to represent the slab by not applying fire load to the top surface of the beam flange (the slab is assumed to prevent heat transfer to the beam below). This approach is used in the remainder of our study since it results in increased computational efficiency and more manageable output file sizes with a negligible effect on the results.

Description of Analyses

This study investigated four analysis cases: (1) both the **b**eams and **c**olumns **u**nprotected—in other words, with no fire protection material (BuCu); (2) **b**eams **p**rotected (in other words, with fire protection) and **c**olumns **u**nprotected (BpCu), (3) **b**eams **u**nprotected and **c**olumns **p**rotected (BuCp); and (4) **b**eams and **c**olumns both **p**rotected (BpCp). These 2-D analyses represent the slab in the model as recommended above. Conventional steel construction requires that fire protection material be applied to both the beams and columns; however, the fire protection material may become dislodged either by a loss of cohesion to the steel over time or due to an event such as a blast or impact. Therefore, the unprotected cases are uncommon but not unrealistic. The unprotected cases represent the conservative envelope of possible behavior, while the protected cases, which assume that the fire protection material has no imperfections and remains intact for the duration of the fire, represents the upper limit of all possible behaviors. In addition to examining the effects of fire protection, these analyses will be used to examine the behavior of steel perimeter columns in a fire.

THERMAL ANALYSIS RESULTS

Figures 8a and 8b show the beam and column thermal analysis results for models BuCu, BpCu, BuCp, and BpCp plotted as the weighted average temperature in the section (considering the mass of the flanges and the web) versus time. Shown are the protected case and the unprotected case for the beam and column on Floor 23, as well as the fire curve used in the analyses. Figure 8a plots this relationship over the entire 43-hour duration of the analysis (which includes a cooling period), whereas Figure 8b plots this relationship for only the first hour. Together, these figures show that the temperatures of the unprotected beam and column sections climbed well over 800 °C (1472 ºF), at which point, based on Eurocode, a 90% reduction in yield strength and modulus of elasticity develops. None of the protected members were heated past 380 °C (716 ºF), indicating that the yield strength of these sections was not reduced by the fire ($k_{y,\theta}$ = 1.0). The modulus of elasticity of the protected member reduced no more than 20% ($k_{E,\theta}$ = 0.80) and 10% for the beam and column, respectively. In addition, these members had a reduced limit of proportionality, $k_{p,\theta}$, equal to 50% for the beam and 15% for the column and would therefore display nonlinear material behavior once their temperature exceeded 100 °C (212 ºF). The unprotected members achieved a much higher average temperature than protected members and their temperature evolution closely resembled the fire curve. The average temperature of the protected beams exceeded the average temperature of the protected columns by about 160 °C (320 ºF) since the beams have only one layer of fire protection material (whereas the columns have two layers) and also because the beams have a smaller mass than the columns. These thermal analysis results were verified by good correlation with an analytical solution based on the lumped mass method (Quiel and Garlock, 2006).

Figure 8b marks the time that the maximum temperatures in the unprotected beam and unprotected column reach 400 ºC (752 ºF), t_b and t_c, respectively (a temperature gradient exists in the sections and therefore the maximum

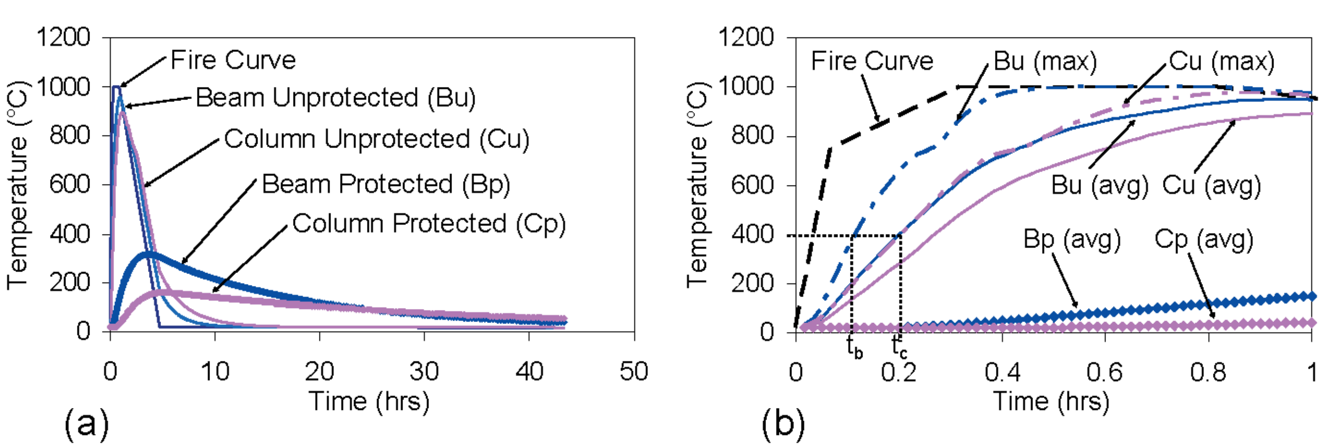

Fig. 8. Applied fire curve and weighted average member temperatures for: (a) the entire time series and (b) the first hour of the fire.

temperature and average temperature do not always coincide). In the paragraphs that follow, these times will be used to correlate structural responses to the time that the material yield strength begins to decrease.

STRUCTURAL ANALYSIS RESULTS

By comparing analysis cases BuCu, BuCp, BpCu, and BpCp, one is able to evaluate the effects of the presence/absence of fire protection material on the structural response of the frame. Analysis cases BuCu, BuCp, and BpCu become unstable (rigid body motions developed and SAFIR failed to converge) before the fire progressed to Floor 23; therefore, the comparative results shown and discussed below are for the beam at Floor 23 and the column between Floors 22 and 23. The analysis with both beams and columns protected (BpCp) survived the entire length of the fire, which is consistent with the 1MP fire event. The following paragraphs describe in detail the results of each analysis.

Figure 9a shows the perimeter column deformation, Δ, magnified 20 times, at Floor 23 of the BuCu frame just before failure, when the fire is burning on Floor 22 only. Figure 9b plots Δ versus time for all four analyses (BuCu, BuCp, BpCu, and BpBp). It is seen that Δ for the analyses with unprotected beams (BuCu and BuCp) is significantly larger than the analyses with protected beams (BpCu, BpCp). On the other hand, the presence/absence of fire protection material on the column does not affect Δ as significantly as the presence/absence of fire protection material on the beam. Note that Δ in the unprotected beam analyses (BuCu and BuCp) decreases even though the fire temperature does not decrease at this time (see Figure 8b). The decrease in Δ is due to the plastic strain and axial shortening in the beam becoming larger than its thermal expansion. This phenomenon is discussed by Quiel and Garlock (2006).

We evaluate the behavior of the beam and column members via two ratios: (1) an axial load ratio defined as the ratio of the analysis axial load to axial yield strength, P/P_y; and (2) a moment ratio defined as the ratio of the analysis moment to the plastic moment capacity, M/M_p. The beam moments are measured at the perimeter column face, whereas the moments in the perimeter column are taken just below Floor 23. All design-oriented load and resistance factors are omitted for these analyses. Yield strength, P_y, and plastic moment, M_p, are obtained at each time step by considering the contributions of each heated fiber in the discretized member cross-sections as follows:

$$P_y = \sum_{i=1}^{n} A_i k_{y,\theta i} \sigma_y \tag{1}$$

$$M_p = \sum_{i=1}^{n} A_i z_i k_{y,\theta i} \sigma_y \tag{2}$$

where

σ_y = yield stress of the steel
A_i = area of each discretized fiber
z_i = distance from the plastic neutral axis to the centroid of each fiber
$k_{y,\theta i}$ = yield stress reduction factor that is computed from the temperature of each fiber

Figures 10a and 10b plot P/P_y and M/M_p, respectively, for the beam on Floor 23 at the exterior column face. Figures 11a and 11b plot P/P_y and M/M_p, respectively, for the column between Floor 22 and Floor 23 at its interface with Floor 23. In addition, Figure 12 shows the axial force (not normalized by P_y) for the beam on Floor 23. These plots include the results of all four fire protection material cases and are used

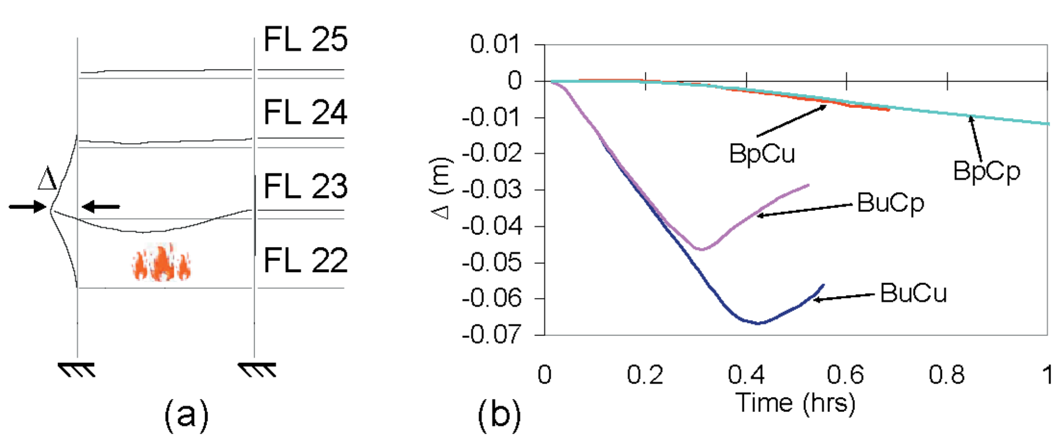

Fig. 9. Column lateral deformation: (a) image (20x) at Floor 23 for BuCu case (grey = undeformed shape) and (b) plotted for all cases on Floor 23.

to evaluate the failure mode of each case as described below. The sign convention is such that positive P represents compression and positive M represents tension on the exterior face of the perimeter column or the top face of the beam.

The analysis case with all members unprotected, BuCu, experiences large reductions in strength in addition to large thermal expansions for both the beams and columns. The BuCu curve in Figure 10a and Figure 11a illustrate increases of the axial load ratio in both the beam and the column, beginning at the time that the material strength decreases (t_b and t_c in Figure 8b). Figure 11b shows that the moment ratio in the column is also significant due to beam expansion which deforms the column and induces large bending moments. The value of M_p begins to decrease at time t_c, in other words, when σ_y begins to be reduced. However, this is not visible in Figure 11b; the M/M_p ratio remains nearly constant between t_c and 14 minutes (marked t_{14} in Figure 11b) since M and M_p are both experiencing slight reductions. The decrease in column moment ratio, occurring at t_{14}, is due to a decrease in axial force in the beam shown in Figure 12, resulting in a column moment. While P/P_y and M/M_p of the beam and column remain below 1.0, a limit state of beam failure is observed as will be described next.

Figure 13a plots (for the BuCu frame) the "pseudo-velocity" (rate of vertical displacement) of the beam mid-span (relative to the column supports) on Floor 23 and of the column at its interface with Floor 23. Figure 13a shows that the pseudo-velocity of the beam increases sharply at 33 min while that of the column remains small, indicating that the beam becomes unstable at which point the analysis terminates. Pseudo-velocity was also used by Usmani et al. (2003) to describe the onset of instability in a building frame.

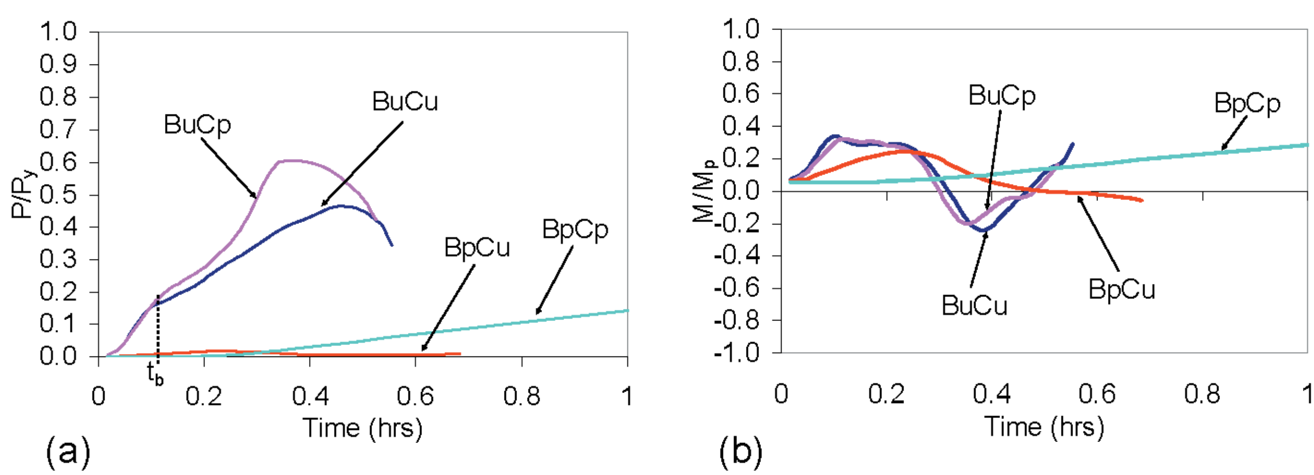

Fig. 10. Computational (SAFIR) results for: (a) axial load ratio and (b) plastic moment ratio for the beam on Floor 23.

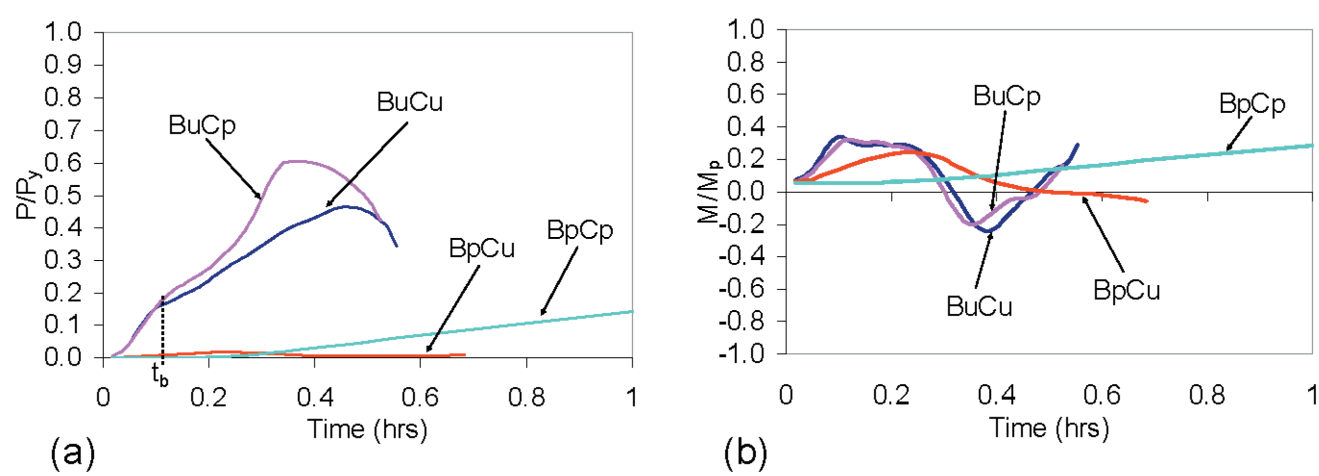

Fig. 11. Computational (SAFIR) results for: (a) axial load ratio and (b) plastic moment ratio for the column just below Floor 23.

To understand how the limit state of beam failure developed, it is necessary to examine the interaction between P and M, as shown in Figure 14a, which plots the path of P/P_y and M/M_p of the beam during the analysis. The combined P and M plastic capacity envelope, which considers the effects of the thermal gradient in the section, is changing with time since the thermal gradient is changing with time. The derivation of this envelope is given in Garlock and Quiel (2006). It is seen that the combined P and M hits the plastic capacity envelope at 31 min and then continues riding this envelope until 33 min when the analysis becomes unstable and the beam is considered to have failed. The plastic capacity envelope at 33 min is negligibly different from the envelope at 31 min and it is not drawn in Figure 14a for clarity.

In the analysis case with beams unprotected and columns protected (BuCp), both the axial load ratio in the beam (Figure 10a) and the moment ratio in the column (Figure 11b) become relatively large. The decrease in column moment at 17 minutes (t_{17}) is due to a decrease in axial force in the beam shown in Figure 12. Figure 13b shows the pseudo-velocity in the beam increases significantly at 32 minutes and then the analysis terminates. An examination of the interaction between the beam P and M, as shown in Figure 14b, reveals that combined P and M lead to beam failure. Figure 14b plots the path of P/P_y and M/M_p of the beam during the analysis. It is seen that as the combined P and M hit the plastic capacity envelope [which is derived according to Garlock and Quiel (2006)] at 23 min, then the points ride the envelope and eventually the analysis terminates at 32 min. The plastic capacity envelope at 32 min is negligibly different from the envelope at 23 min and it is not drawn in Figure 14b for clarity.

The BuCp analysis becomes unstable and terminates about 1 min before the BuCu analysis. This trend is due to a larger axial force developing in the BuCp beams than the BuCu beams as shown in Figure 10a. Since a fire protected

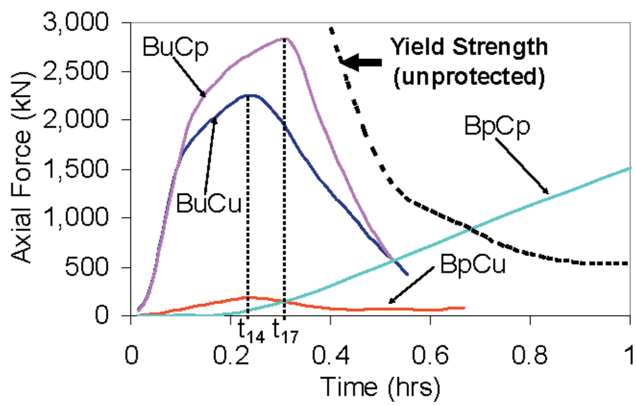

Fig. 12. Axial force in the beam on Floor 23, measured at its interface with the perimeter column.

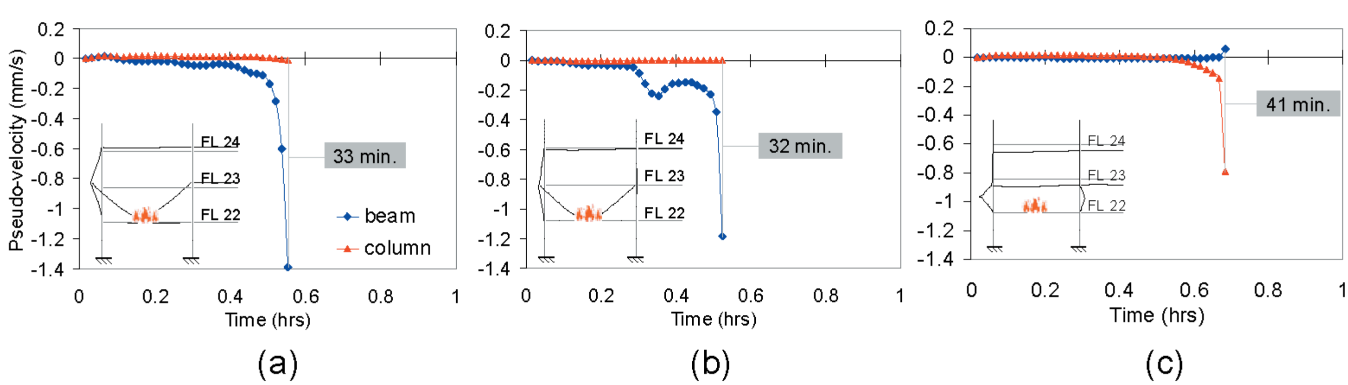

Fig. 13. Rate of vertical displacement (pseudo-velocity) in the column at the Floor 23 interface and in the beam at midspan (relative to the column) for: (a) BuCu, (b) BuCp, and (c) BpCu analysis cases. Final deformed shapes (20x) are included.

column (analysis BuCp) is stiffer than an unprotected column (analysis BuCu), the protected column provides more axial restraint to the beam, which results in larger axial forces in the beam. In any case, the difference in failure time and beam and column behavior between analyses BuCu and BuCp is not significant.

In the BpCu case, the columns suffered a significant reduction in axial yield strength. As this strength diminished, the axial load ratio in the column became large, climbing to a value near 0.9 as seen in Figure 11a. This increase in the axial load ratio was due to a significant reduction in σ_y beginning at time t_c. Figure 11b shows that the moment ratio in the column is also significant. The decrease in column moment at time t_{14} is correlated to a decrease in axial force in the beam shown in Figure 12. Figure 13c shows that the pseudo-velocity of the column increases sharply at 41 min, while the pseudo-velocity of the beam remains very small throughout the analysis. The failure mode for this case is combined column axial yielding and bending due to a reduction in material strength under high temperatures. Figure 14c plots the path of P/P_y and M/M_p of the column during the analysis. The combined P and M plastic capacity envelope, which is derived by Garlock and Quiel (2006), at the time of failure is drawn. It is seen that when the analysis hits this envelope the analysis terminates. Failure in this analysis case is controlled by the column strength under combined P and M. Figure 13c shows the final deformed shape of the frame at failure (magnified 20 times), visually confirming a column failure mode.

The BpCp analysis survived the entire duration of the 18.5-hour fire, which is consistent with the actual behavior of our prototype building. The axial loads and moments in the beam remained relatively small throughout the analysis for the first hour of the fire (see Figure 10). In the columns, the axial load ratio also remained small (see Figure 11a); however, a plastic hinge was formed shortly after one hour primarily due to a large M/M_p (due to beam thermal expansion which induced column deformation) combined with a relatively small P/P_y. About one hour later, the column moments decreased as the fire progressed up the building. This behavior did not result in structural instability since a collapse mechanism (the formation of several plastic hinges in the columns leading to instability) did not form. The results shown in Figures 10 and 11 are for Floor 23 yet the behavior of other floors was similar.

Figure 15 shows the deformed structure at three intervals of the time series analysis. Figure 15a represents t = 6.5 hours when the fire has reached its maximum intensity

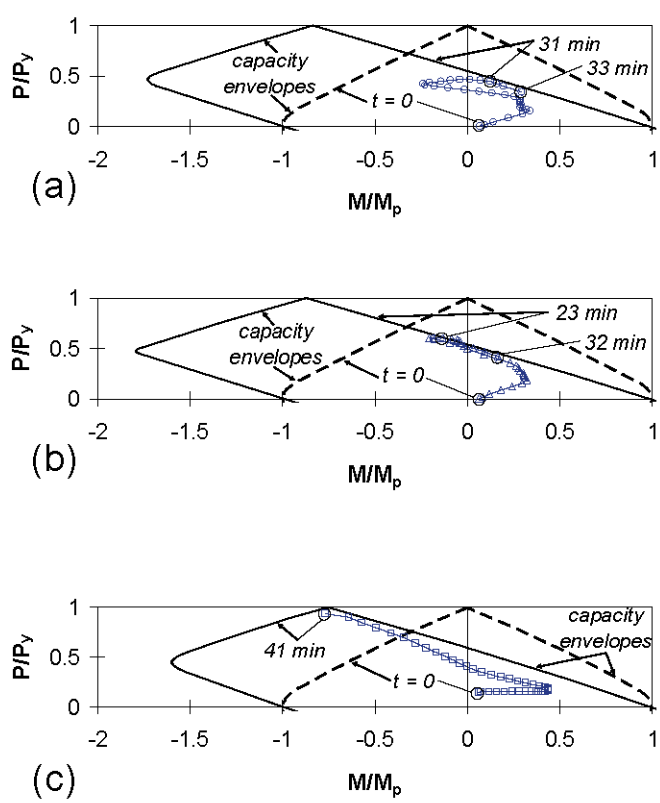

Fig. 14. Combined normalized axial load-moment interaction of: (a) the Floor 23 beam in analysis BuCu; (b) the Floor 23 beam in analysis BuCp; and (c) the Floor 22-23 column in analysis BpCu.

on Floor 25 and is still burning on Floor 24 and, to a lesser extent, on Floor 23 (see Figure 2). Figure 15b represents t = 18.5 hours, when the fire has been extinguished on Floor 30 yet some of the structure is still hot and therefore deformed. During the fire, the maximum column lateral deformation was approximately 43 mm (1.7 in.) on Floors 28 though 30. Figure 15c represents t = 37.5 hours at the end of the cooling period, where it is seen that almost all of the structure has returned to its original position with negligible residual deformations [this BpCp behavior is possible since the material model is assumed to be reversible (Franssen, 1990)]. The residual deformations that remained in the column were within construction tolerances of *height*/500.

ANALYSIS RESULTS IN CONTEXT OF FULL-SCALE FIRE EXPERIMENTS ON STEEL FRAMES

In this section, the results of our 2-D study are placed in the context of fire experiments, which were performed at the Building Research Establishment's (BRE) Cardington laboratory, on three-dimensional (3-D) steel frames (Bailey, Lennon, and Moore, 1999). The steel frame was eight stories tall with wide-flanged sections and it included the floor slab, which was designed to act compositely with the beams. The beam and column sizes were smaller than those implemented in the prototype presented in this paper since the Cardington steel frame was not as tall and was constructed to carry gravity loads only (not as a MRF). All columns were protected and all beams were unprotected (which is analogous to the BuCp analysis of our study). These tests showed that after the steel beams lost most or all of their strength, floor collapse did not develop due to the composite slab's ability to support the load in tensile membrane action. Such behavior cannot be captured in a 2-D analysis, and one must therefore consider such an analysis to be conservative in this context. However, failure of a beam that laterally braces a perimeter column will jeopardize the structural integrity of that frame, even if the slab continues to carry the gravity loads. Although a 2-D analysis cannot predict slab membrane failure (floor collapse), it can indicate beam failure which represents a potentially critical structural condition.

One of the first Cardington experiments did not protect the columns above the false ceiling, leaving a short length of 400 mm (15.7 in.) unprotected. In this test, the short unprotected length of the column was squashed and brought down all the floors above this column the amount of the squashing deflection, thus leading to damage that was disproportionate to the cause (Wang and Kodur, 2000). The BpCu analysis of the current study also shows that when the column fails, the resulting damage is global (it affects all floors above). Both

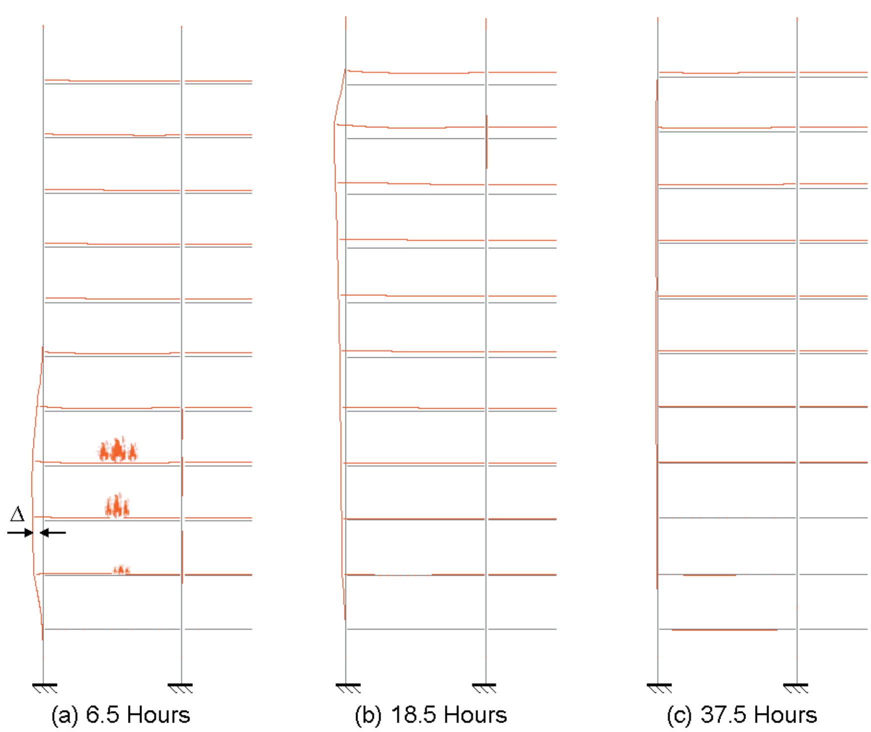

Fig. 15. Deformed shape (20x) of the BpCp frame: (a) during the fire; (b) at the end of the fire; and (c) at the end of the cooling period (grey = undeformed shape).

the Cardington tests and the current study therefore point to the importance of column strength to overall structural integrity. The current study, in particular, also emphasizes the role that the beams play on the strength of perimeter columns. The thermal expansion of the beams and the thermal gradients in the perimeter columns induce large moments in the perimeter columns. Such large moments in the perimeter columns were also observed in the Cardington tests, even though the structural behavior that generated those moments was not well understood at the time (Bailey, Lennon, and Moore, 1999).

SUMMARY AND CONCLUSIONS

This study investigated the thermal and structural effects of the slab and fire protection material on the perimeter columns of a steel high-rise building exposed to fire. The beam sizes, column sizes, and applied fire remained constant in the prototype frames, but the presence/absence of fire protection material and the method of representing the slab varied. Our study indicated that in 2-D analyses it is reasonable to represent the slab in the thermal and structural model by not applying fire load to the top surface of the steel beam flange (the slab is therefore assumed to prevent heat transfer to the beam below).

In the analyses with unprotected beams, the beams achieved higher temperatures, which lead to greater thermal expansions and therefore larger column lateral deformations than the cases with the beams protected. With no fire protection material on either the beams or columns (or both), the frame became unstable within an hour of the fire's ignition. If fire protection material is applied to both the beams and columns (as specified by the building's construction documents), the structure survives the full duration of the fire.

The fire-induced structural response of the beams that frame into the perimeter column directly affects the perimeter column behavior and structural integrity of the frame in the following ways:

(1) As these beams are heated, they expand and force the column to deform laterally, which induces large column moments that combine with large axial gravity forces to create a plastic hinge. This behavior does not necessarily result in structural instability since a collapse mechanism (the formation of several plastic hinges in the columns leading to instability) may not form.

(2) If the beams do not have fire protection material, they reach their capacity due to bending and the fire-induced axial forces that develop in them. Once these beams, which brace the perimeter column, fail, the stability of the column, and structure as a whole, may be compromised and could potentially lead to structural collapse.

Both this study and full-scale tests of steel frames have shown that the strength of the columns is vital, and therefore the appropriate steps should be taken to adequately protect them against fire exposure. However, especially in the case of the perimeter column, one must also carefully consider the design and fire protection of the members that brace them (the beams). It is therefore recommended that the fire protection material requirements for the beams bracing the perimeter columns be larger than that of the other beams in the building since they significantly affect the perimeter column behavior and have the potential to compromise overall frame stability. The results presented in this paper therefore support the fire protection methodology of current IBC Type 1A construction (ICC, 2000), which requires beams that frame into columns to have the same level of fire protection (3 hours) as the columns to which they connect. Older construction, which required less fire protection to these critical beams than the columns (as was the case for our prototype), should be considered for upgrading to meet current codes. More research is needed to determine recommended levels of fire protection material for these beams. While fire resistive material is important in steel structures, the One Meridian Plaza event (our prototype for this study) also demonstrates the importance of automatic sprinkler systems. The floors in our prototype that were engulfed by the fire did not have operational sprinklers, which can control and extinguish fires before they reach the dangerous post-flashover stage.

When a beam or column limit state was reached in the analyses, it was reached by the combined action of axial load and moment. The beams and columns examined in this study act as beam-columns (members that are subject to both axial load and moment), and therefore their capacity and behavior should be examined with this perspective.

ACKNOWLEDGMENTS

Mr. Quiel has been involved with this research project while on appointment as a U.S. Department of Homeland Security (DHS) Fellow under the DHS Scholarship and Fellowship Program, a program administered by the Oak Ridge Institute for Science and Education (ORISE) for DHS, through an interagency agreement with the U.S Department of Energy (DOE). ORISE is managed by Oak Ridge Associated Universities under DOE contract number DE-AC05-00OR22750. All opinions expressed in this paper are the author's and do not necessarily reflect the policies and views of DHS, DOE, or ORISE.

REFERENCES

ACI (2002), *Building Code Requirements for Structural Concrete (ACI 318-02) and Commentary (ACI 318R-02)*, American Concrete Institute, Farmington Hills, MI.

AISC (2005), *Specification for Structural Steel Buildings*, ANSI/AISC 360-05, American Institute of Steel Construction, Inc., Chicago, IL.

ASCE (2005), *Minimum Design Loads for Buildings and Other Structures*, ASCE/SEI 7-05, American Society of Civil Engineers, Reston, VA.

Bailey, C.G., Lennon, T., and Moore, D.B. (1999), "The Behavior of Full-Scale Steel-Framed Buildings Subjected to Compartment Fires," *The Structural Engineer*, Vol. 77, No. 8, pp. 15–21.

BOCA (1969), *The BOCA Basic Building Code 1970*, Fifth Edition, Building Officials and Code Administrators International, Inc., Chicago, IL.

Buchanan, A.H. (2002), *Structural Design for Fire Safety*, John Wiley & Sons, Chicester, U.K.

Culver, C.G. (1976), "Live-Load Survey Results for Office Buildings," *Journal of the Structural Division*, ASCE, Vol. 102, No. ST12, pp. 2269–2284.

Dexter, R.J. and Lu, L.-W. (2001), "The Effects of a Severe Fire on the Steel Frame of an Office Building," *Engineering Journal*, AISC, Vol. 38, No. 4, pp. 167–175.

EC1 (1994), *Eurocode 1: Basis of Design and Design Actions on Structures. Part 2-2: Actions on Structures Exposed to Fire*, ENV 1991-2-2, CEN, Brussels, Belgium.

EC3 (2001), *Eurocode 3: Design of Steel Structures. Part 1.2: General Rules—Structural Fire Design*, ENV 1993-2-2:2001, CEN, Brussels, Belgium.

FEMA (1991), *High-rise Office Building Fire: One Meridian Plaza, Philadelphia, Pennsylvania*, USFA Technical Report Series, FEMA, Washington, DC.

Franssen, J.-M. (1990), "The Unloading of Building Materials Submitted to Fire," *Fire Safety Journal*, Vol. 16, pp. 213–227.

Franssen, J.-M. and Gens, F. (2004), "Dynamic Analysis Used to Cope with Partial and Temporary Failures," *Proceedings of the Third International Workshop for Structures in Fire*, Ottawa, Ontario, May 10–11, Franssen, Benichou, Kodur & Sultan ed., pp. 297–308.

Franssen, J.-M. (2005), "SAFIR: A Thermal/Structural Program for Modeling Structures Under Fire," *Engineering Journal*, AISC, Vol. 42, No. 3, 143–158.

Garlock, M.E.M. and Quiel, S.E. (2006), "Combined Axial Load and Moment Capacity of Fire-Exposed Beam-Columns with Thermal Gradients," *Proceedings of the Fourth International Workshop for Structures in Fire*, Aviero, Portugal, May 10–12, Vila Real, Franssen & Lopes ed., Vol. 1, pp. 187–198.

ICC (2000), *The 2000 International Building Code (IBC 2000)*, International Code Council, Falls Church, VA.

Kawagoe, K. (1958), "Fire Behavior in Rooms," *Report No. 27*, Building Research Institute, Ministry of Construction, Tokyo.

Kirby, B.R., Wainman, D.E., Tomlinson, L.N., Kay, T.R., and Peacock, B.N. (1999), "Natural fires in large scale compartments," *International Journal on Engineering Performance-Based Fire Codes*, Hong Kong Polytechnic University, Construction Industry Development, Studies and Research Centre, FA.

Klem, T.J. (1991), "High-Rise Fire Claims Three Philadelphia Fire Fighters," *NFPA Journal*, National Fire Protection Association, September/October.

McGrattan, K.B., Bouldin, C., and Forney, G.P. (2005), "Computer Simulation of the Fires in the World Trade Center Towers," *NIST NCSTAR 1-5F*, National Institute of Standards and Technology, Gaithersburg, MD.

NIST (2004), "Appendix M: Interim Report on 2-D Analysis of WTC Towers Under Gravity Load and Fire," *Progress Report on the Federal Building and Fire Safety Investigation of the World Trade Center Disaster*, NIST Special Publication 1000-5, National Institute of Standards and Technology, Gaithersburg, MD, June 2004.

Quiel, S.E. and Garlock, M.E.M. (2006), "A Performance-Based Design Approach for Steel Perimeter Columns Subject to Fire," *Proceedings of the Fourth International Workshop for Structures in Fire*, Aviero, Portugal, May 10–12, Vila Real, Franssen & Lopes ed., Vol. 1, pp. 175–186.

Usmani, A.S., Chung, Y.C., and Torero, J.L. (2003), "How did the WTC towers collapse: a new theory," *Fire Safety Journal*, Vol. 38, pp. 501–533.

Wang, Y.C. and Kodur V.K.R. (2000), "Research Toward Use of Unprotected Steel Structures," *Journal of Structural Engineering*, ASCE, Vol. 126, No. 12, pp. 1442–1450.

Zarghamee, M.S., Bolourchi, S., Eggers, D.W., Erbay, O.O., Kan, F.W., Kitane, Y., Liepins, A.A., Mudlock, M., Naguib, W.I., Ojdrovic, R.P, Sarawit, A.T., Barrett, P.R., Gross, J.L., McAllister, T.P. (2005), "Component, Connection, and Subsystem Structural Analysis," *NIST NCSTAR 1-6*, National Institute of Standards and Technology, Gaithersburg, MD.